Ab Initio Calculations on Reactions of CHF_3 with Its Fragments

Yasuharu Okamoto* and Mutsumi Tomonari

Fundamental Research Laboratories, NEC Corporation, Tsukuba, Ibaraki 305-8501, Japan

Received: September 3, 1999; In Final Form: January 3, 2000

Using ab initio calculations, CHF_3 decomposition and CHF_3-related reactions denoted generally as $CHF_3 + X \rightarrow$ products were examined. As species X, we considered CHF_3 itself and its fragments (CF_3, CHF_2, CF_2, CHF, CF, CH, F, and H). These reactions are polymerizations, abstractions by radicals, and insertions of radicals into a C−H or a C−F bond of the CHF_3 molecule. Although abstractions occur with low reaction barriers, polymerizations and insertions that increase the number of C atoms have a large reaction barrier with the exceptions of CHF, CF, or CH radical insertions.

Introduction

Global warming is one of the gravest issues concerning the earth's environment. Although a large part of global warming is thought to have been caused by an increased concentration of CO_2 gas in the atmosphere—from 280 ppm before the Industrial Revolution to 360 ppm now—other greenhouse gases such as perfluorocarbons (PFCs) and hydrofluorocarbons (HFCs) may have also contributed. The global warming potentials (GWPs) of PFCs and HFCs are typically 1000−10 000 times as high as that of CO_2 (whose GWP is 1) because of their high infrared absorbency and long atmospheric lifetimes.[1] For example, the GWPs of CF_4 and C_2F_6 molecules are 9200 and 6500, respectively.[1] Thus, the release of such gases should be reduced.

In the semiconductor industry, PFCs and HFCs are used in various device-fabrication processes such as etching, cleaning, and deposition. Among the HFCs, CHF_3 is the simplest molecule and is commonly used as an etchant of SiO_2 films.[2] However, although CF_4 and C_2F_6 molecules, which are major components of gases emitted from the etching process,[3] can be collected by membrane separation,[4] CHF_3, which is another main component,[3] is not captured because of the smallness of the CHF_3 molecule.[4] Becaeuse CHF_3 has a very large GWP of 11 700,[1] the recycling of CHF_3 gas is urgently needed.

If the CHF_3 molecule is converted into molecules that can be captured by membrane separation, the emission of high GWP gases into the atmosphere can be reduced. Thus, as a first step toward such a goal, a systematic examination of gas-phase reactions related to CHF_3 will provide valuable information concerning the possible conversion of CHF_3 and will help control the emission of high GWP gases. We have performed ab initio calculations to elucidate these elementary reactions, which may also help deepen our fundamental knowledge of fluorocarbon chemistry.

We have investigated the decompositions of CHF_3 and CHF_3—related reactions that are generally written as $CHF_3 + X \rightarrow A + B$. As species X, we considered CHF_3 itself and its possible fragment species (CF_3, CHF_2, CF_2, CHF, CF, CH, F, and H). These reactions are polymerizations of CHF_3, abstractions by radicals (CF_3, CHF_2, F, and H), and insertions of radicals (CF_2, CHF, CF, and CH) into a C−H or a C−F bond of the CHF_3 molecule. We focused particularly on polymerization and insertion reactions because an increased number of C atoms may facilitate capture through a membrane separation technique because of an enlarged molecular size.

Computational Method

In the calculations, we used an ab initio molecular orbital method at the levels of the hybrid-density-functional theory (DFT) and the second-order Möller−Plesset perturbation theory (MP2). The B3LYP scheme was used as the exchange-correlation functional for hybrid-DFT.[5−8] The stable molecular structures and transition states (TSs) were determined by both methods (B3LYP and MP2) using the 6-31++G(d′,p′) basis set.[9] The total energies of these optimized structures were corrected by calculation with the larger 6-311++G(2df,p) basis set for both methods.

The reaction energy (E_R) was defined as $E_R = E$(reactant) − E(product), unless otherwise stated. Zero-point-energy (ZPE) correction was carried out at the B3LYP/6-31++G(d′,p′) level. (The MP2 calculation of the ZPE was much too demanding computationally. Moreover, the ZPE is less sensitive than the total energy to the method used.[10]) The G2[11] and G3MP2 methods,[12,13] which provide thermochemical properties with high accuracy, were also used to examine the CHF_3-related reactions, and the results were compared with those obtained by the B3LYP and MP2 methods.

For the polymerization and insertion reactions, the Gibbs free-energy change ($\Delta G \equiv \Delta H - T\,\Delta S$, where T, H, and S are temperature, enthalpy, and entropy, respectively) was calculated at 200−1000 K (with increments of 100 K). The vibrational contribution to the Gibbs energy was calculated at the B3LYP/6-31++G(d′,p′) level. All calculations were done using the GAUSSIAN94[14] and GAUSSIAN98[15] programs installed on NEC-SX4 supercomputing systems.

Results and Discussion

Thermochemistry of CHF_3 Decomposition. First, we examined the CHF_3 decomposition (D1−D9 in Table 1). Although fragmentation of the molecule is caused by electron collisions in plasma etching,[16,17] an understanding of the thermochemistry at each decomposition step will help us to determine the fragmentation pathways.

Among the C−F bond-breaking reactions (D2, D3, D5, D6, and D8), the D3 and D5 reactions need less energy for bond dissociation than the other reactions which require from 5.42 to 5.57 eV (G2 method). The C−F bond observed in the D3

10.1021/jp993134b CCC: $19.00
Published on Web 02/29/2000

TABLE 1: Reaction Energy[a] [in eV] of the CHF_3 Decomposition Calculated at the G2, G3MP2, B3LYP (B3LYP/6-311++G(2df,p)//B3LYP/6-31++G(d′,p′)), and MP2 (MP2/6-311++G(2df,p)//MP2/6-31++G(d′,p′)) Levels of Theory

reaction	G2	G3MP2	B3LYP[b]	MP2[b]
D1: $CHF_3 \rightarrow CF_3 + H$	−4.62	−4.56	−4.41	−4.36
D2: $CHF_3 \rightarrow CHF_2 + F$	−5.57	−5.45	−5.21	−5.65
D3: $CF_3 \rightarrow CF_2 + F$	−3.59	−3.58	−3.66	−3.94
D4: $CHF_2 \rightarrow CF_2 + H$	−2.65	−2.69	−2.86	−2.65
D5: $CHF_2 \rightarrow CHF + F$	−4.79	−4.80	−4.90	−5.20
D6: $CF_2 \rightarrow CF + F$	−5.42	−5.30	−5.19	−5.52
D7: $CHF \rightarrow CF + H$	−3.27	−3.20	−3.12	−2.98
D8: $CHF \rightarrow CH + F$	−5.49	−5.37	−5.32	−5.58
D9: $CHF_3 \rightarrow CF_2 + HF$	−2.36 (3.20)[c]	−2.27 (3.18)	−2.33 (2.94)	−2.48 (3.18)

[a] In the reaction energies, minus means the reaction is endothermic. [b] Zero-point vibrational energies were evaluated by B3LYP/6-31++G(d′,p′). [c] The figures in parentheses show the activation energies.

TABLE 2: Reaction[a] (Activation) Energies [in eV] of the Elementary Processes Calculated at the B3LYP, MP2, and G3MP2 Levels of Theory

	reaction	B3LYP[b]	MP2[c]	G3MP2
R1	$CHF_3 + CHF_3 \rightarrow C_2F_6 + H_2$	−0.58 (6.33)	−0.36 (6.51)	−0.36 (5.53)
R2	$CHF_3 + CHF_3 \rightarrow C_2HF_5 + HF$	−0.18 (4.14)	−0.01 (4.54)	0.02 (4.50)
R3	$CHF_3 + CF_3 \rightarrow CF_3 + CHF_3$	0.0 (0.51)	0.0 (0.75)	0.0 (0.67)
R4	$CHF_3 + CF_3 \rightarrow CHF_2 + CF_4$	0.09 (1.73)	0.12 (2.52)	0.13 (2.16)
R5	$CHF_3 + CF_3 \rightarrow C_2F_6 + H$	−0.66 (3.74)	−0.10 (4.05)	−0.32 (3.72)
R6	$CHF_3 + CHF_2 \rightarrow CF_3 + CH_2F_2$	−0.20 (0.60)	−0.22 (0.87)	−0.22 (0.79)
R7	$CHF_3 + CHF_2 \rightarrow CHF_2 + CHF_3$	0.0 (1.74)	0.0 (2.46)	0.0 (2.19)
R8	$CHF_3 + CF_2 \rightarrow C_2HF_5$	2.15 (2.51)	2.47 (2.75)	2.28 (2.78)
R9	$CHF_3 + CHF \rightarrow CHF_2CHF_2$	3.33 (1.70)	3.62 (1.81)	3.40 (1.91)
R10	$CHF_3 + CHF \rightarrow CH_2FCF_3$	3.57 (0.30)	3.92 (0.39)	3.67 (0.66)
R11	$CHF_3 + CF \rightarrow CF_3CHF$	2.45 (no[d])	2.68 (no)	2.49 (no)
R12	$CHF_3 + CF \rightarrow CHF_2CF_2$	2.19 (no)	2.32 (no)	2.15 (no)
R13	$CHF_3 + CH \rightarrow CF_3CH_2$	4.37 (0.08)	4.65 (0.21)	4.32 (0.14)
R14	$CHF_3 + CH \rightarrow CHF_2CHF$	3.62 (1.60)	3.89 (1.82)	3.62 (1.88)
R15	$CHF_3 + H \rightarrow CF_3 + H_2$	0.08 (0.33)	−0.26 (0.87)	−0.03 (0.62)
R16	$CHF_3 + H \rightarrow CHF_2 + HF$	0.52 (1.34)	0.17 (2.17)	0.43 (1.77)
R17	$CHF_3 + F \rightarrow CF_3 + HF$	0.93 (no)	1.06 (no)	1.32 (no)
R18	$CHF_3 + F \rightarrow CHF_2 + F_2$	−3.70 (no)	−4.01 (no)	−3.90 (no)

[a] In the reaction energies, minus means the reaction is endothermic. [b] B3LYP/6-311++G(2df,p)//B3LYP/6-31++G(d′,p′) + ZPVE(B3LYP/6-31++G(d′,p′)). [c] MP2/6-311++G(2df,p)//MP2/6-31++G(d′,p′) + ZPVE(B3LYP/6-31++G(d′,p′)). [d] *no* means that a transition state was not found in the elementary process.

and D5 reactions is relatively weak. On the other hand, among the C−H bond-breaking reactions (D1, D4, and D7), the bond energy of D4 is significantly smaller than that of the other reactions.

Ricca[18] calculated the heats of formation for CF_n ($n = 1-4$) by coupled cluster singles and doubles including a perturbational estimate of the triplet excitation (CCSD(T)) combined with extrapolation to the complete basis set (CBS) limit. The bond energies of CF_2-F and CF−F calculated by CBS−CCSD(T) were 3.73 and 5.46 eV,[18] which agree well with our results (Table 1). Our calculations on the bond dissociation energies of CF_2-F and CF−F molecules by QCISD(T)/6-311+G(2df)//MP4SDQ/6-311+G(2d) (CCSD(T)/6-311+G(2df)//MP4SDQ/6-311+G(2d)) are 3.67 eV (3.67 eV) and 5.30 eV (5.30 eV), respectively. These results may suggest that the accuracy of the G2 and G3MP2 methods is about 0.15 eV.

The square root deviations from the G2 reaction energy of the B3LYP and MP2 methods $({}^1/_9\sqrt{\sum(E_R(\mathrm{D}n\text{: G2}) - E_R(\mathrm{D}n\text{: X}))^2}$, X = B3LYP or MP2) are respectively 0.065 and 0.077 eV, which confirm that both methods provide fairly reliable thermochemical values. Moreover, the maximum absolute deviation from the G2 reaction energy of B3LYP is 0.36 eV in reaction D2 (where MP2 predicts a value close to that obtained by the G2 method) and the maximum absolute deviation of MP2 from G2 is 0.41 eV in reaction D5 (where B3LYP predicts a value close to that obtained by the G2 method). For predicting the energy, B3LYP and MP2 methods complement each other. On the other hand, G3MP2 calculations are much closer to G2 calculations than above B3LYP and MP2 methods. The square root deviation of G3MP2 from the G2 reaction energy is 0.027 eV, and the maximum absolute deviation of G3MP2 from G2 is 0.12 eV in reaction D2.

Reaction D9 is an elimination of a HF molecule from CHF_3. Because the activation energy of D9 is lower than the dissociation energies of D1 and D2, HF elimination may be an important pathway for the CHF_3 decomposition.

CHF_3 Reactions with Itself and Its Fragments. Next, we examined the CHF_3 reactions with CHF_3 and its fragment species (CF_3, CHF_2, CF_2, CHF, CF, CH, F, and H). The reaction energies and activation energies (if any) are listed in Table 2, and the molecular geometries at the TSs are shown in Figure 1.[19] In the following, we discuss the characteristics of each reaction.

Reactions R1 and R2 are a direct polymerization of CHF_3 molecules. Although R2 is a more favorable reaction than R1, both kinematically and thermodynamically, the reaction barrier of R2 is still high. Therefore, these direct polymerizations of CHF_3 molecules are unlikely to occur.

Reactions R3 and R4 are abstractions by a CF_3 radical. Because the products of R3 are the same as the reactants, R3 leads to no change. The reaction barrier of R4 is significantly higher than that of R3, which corresponds to a C−F bond energy being larger than a C−H bond energy (Table 1). This analysis also applies to R6 and R7 where CHF_2 abstracts H (R6) or F (R7) from CHF_3. However, in that case R6, which has a lower

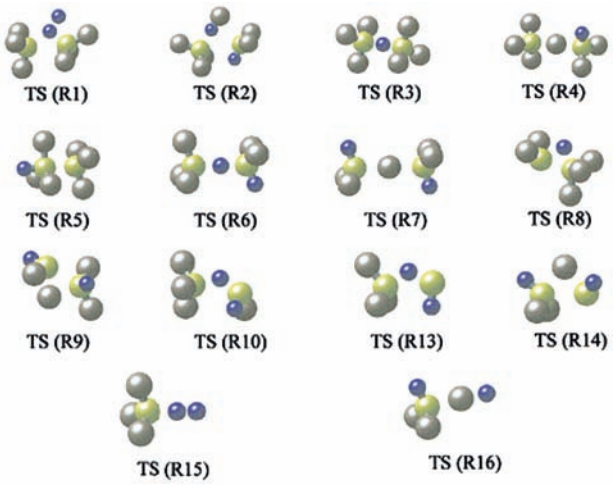

Figure 1. Transition states (TSs) of CHF_3-related reactions determined by B3LYP/6-31++G(d′,p′). Yellow, brown, and purple balls respectively stand for C, F, and H atoms.

reaction barrier, is a thermodynamically less favorable process than R7.

Reactions R8−R10 are insertions of methylene derivatives (CXY: CF_2 or CHF) into a C−H bond (R8 and R10) or a C−F bond (R9) of the CHF_3 molecule. All of these are exothermic reactions. Because the reaction barriers of R9 and R10 are lower than that of R8, CHF is more reactive than CF_2. Because a C−H bond is weaker than a C−F bond, R10 has a lower reaction barrier than R9. This is also true of two pair reactions: (R13, R14).

Reactions R11 and R12 are insertion of a CF radical into a C−H bond (R11) or a C−F bond (R12), and reactions R13 and R14 are insertions of a CH radical into a C−H bond (R13) or a C−F bond (R14). Although the CH insertions have TSs, we could not find TSs for the CF insertions.

By comparing the pair reactions (R9, R10), (R11, R12), and (R13, R14), we found that the species that have a $-CF_3$ group are thermodynamically favorable products that have a polarized C−C bond ($C(\delta^-)HXY-C(\delta^+)F_3$). This bond becomes short due to the polarization effect. For example, Mulliken populations on carbon atoms of CHF_2-CHF_2 and CH_2F-CF_3 molecules calculated by the B3LYP are $C(+0.11)HF_2-C(+0.11)HF_2$ and $C(-0.15)H_2F-C(+0.51)F_3$, respectively. The length of a C−C bond of a CHF_2-CHF_2 molecule is 1.532 Å, whereas that of a CH_2F-CF_3 molecule is 1.524 Å. MP2 calculation gives qualitatively the same results as the B3LYP: it provides the values $C(+0.22)HF_2-C(+0.22)HF_2$ and $C(-0.11)H_2F-C(+0.72)F_3$ for the Mulliken charge and 1.525 and 1.518 Å, respectively for the C−C bonds.

Reactions R15 and R16 are abstractions by a H radical. As was often observed in the above results, R16, which includes the C−F bond breaking, has a higher reaction barrier than R15. However, R16 is thermodynamically more favorable than R15.

Reactions R17 and R18 are abstractions by a F radical. Contrary to the above abstractions by a H radical, these reactions have no TS; i.e., the reaction is simply attractive (R17) or repulsive (R18), as we confirmed by examining the potential energy curves and the C−H (C−F) distance while taking a H−F (R17) or a F−F (R18) as a reaction coordinate (Figure 2).

The mean absolute difference of the reaction energy between B3LYP and G3MP2 is 0.13 eV, which is smaller than that between MP2 and G3MP2 (0.17 eV). On the other hand, the mean absolute difference of the activation energy between B3LYP and G3MP2 is 0.31 eV, which is larger than that between MP2 and G3MP2 (0.24 eV).

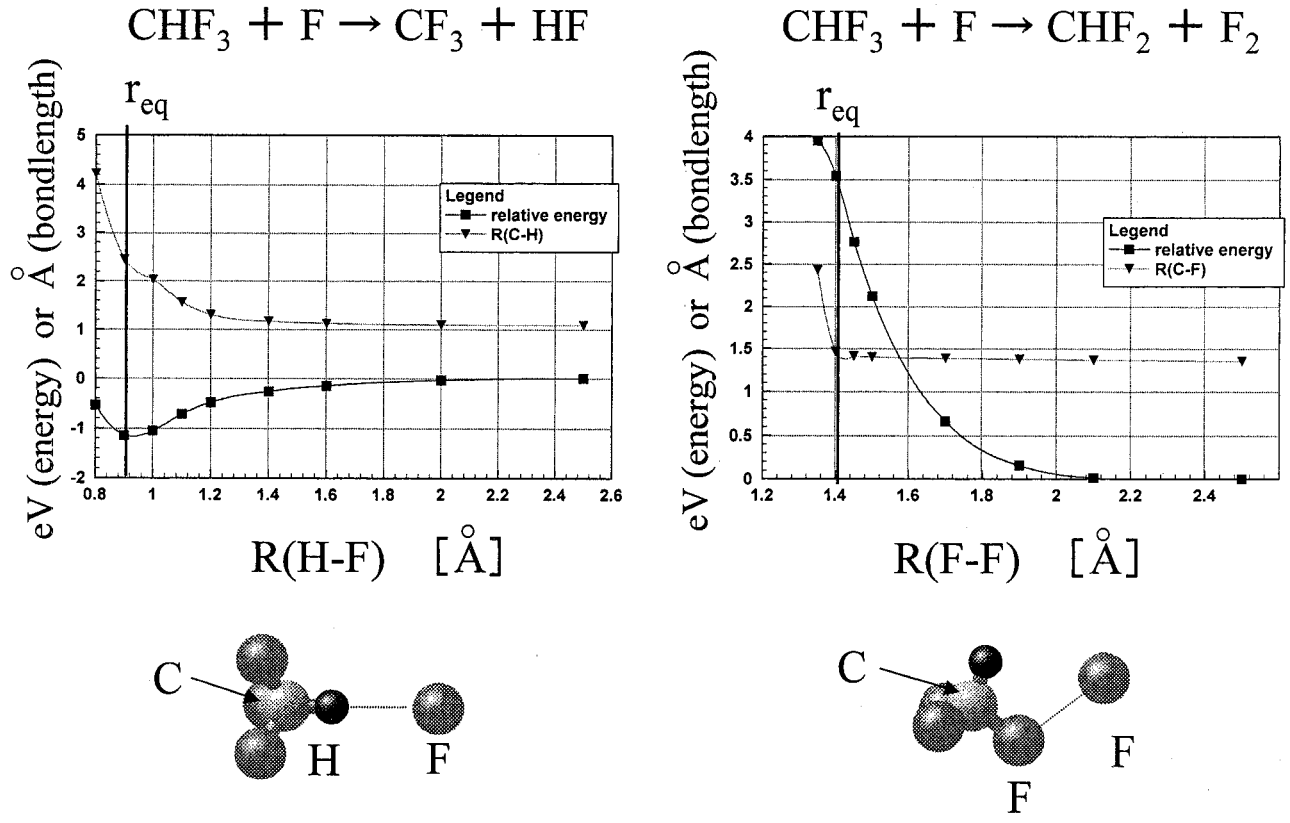

Figure 2. Potential energy curve and C−H (C−F) distance of reaction R17 (left) and R18 (right) obtained by B3LYP/6-31++G(d′,p′). r_{eq} stands for the equilibrium bond length of HF (left) and F_2 (right) molecules.

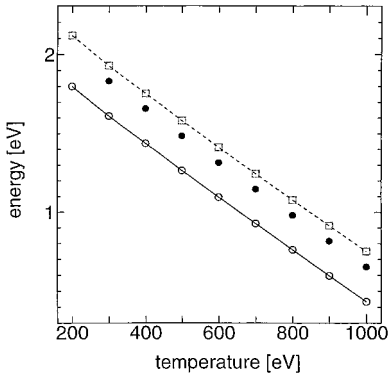

Figure 3. Gibbs energy change of reaction: $CF_4 + CF_2 \rightarrow C_2F_6$ at 200−1000 K. White circles and squares stand for B3LYP and MP2 results, respectively. Black circles are values obtained from a thermochemical data book.[20] In this and Figures 4 and 5, the lines are only guides for the eye.

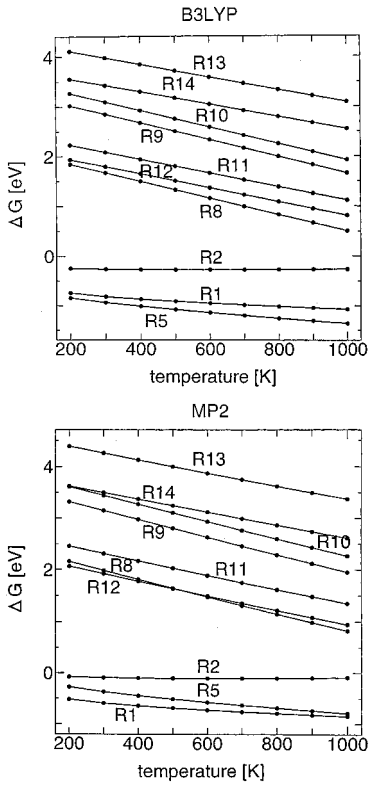

Figure 4. Gibbs energy change of reaction (R1, R2, R5, and R8−R14) at 200−1000 K obtained by B3LYP (top) and MP2 (bottom).

Gibbs Energy Change in Reactions Where the Carbon Number Increases. Finally, for reactions that increase the number of C atoms (i.e., R1, R2, R5, and R8−R14), we calculated the Gibbs energy change for reaction energies and reaction barriers at 200−1000 K (with increments of 100 K). To assess the reliability of our computational scheme, we calculated the Gibbs energy change of the reaction $CF_4 + CF_2 \rightarrow C_2F_6$ and compared the result with the value obtained from a thermochemical data book.[20] Figure 3 shows that these reference values from thermochemical data lie between the B3LYP and MP2 calculations. Thus, the present computational scheme is fairly reliable (about −0.2 to ∼0.1 eV).

Figure 4 shows the Gibbs energy change for reaction energies. Both B3LYP and MP2 predict similar trends. R1, R2, and R5 are endothermic and the others are exothermic reactions irrespective of temperature. Reactions R8−R14 reduce the number of molecules from two in the reactant to one in the product, which is disadvantageous for the entropy term. Thus, these reactions become less exothermic as the temperature increases. This analysis also applies to the activation energy, where the barrier heights increase as the temperature increases (Figure 5). In addition to the barrierless reactions of R11 and R12, only R10 and R13 have low activation energies. The reactions that increase the number of C atoms, other than R10−R13, seem unlikely to occur in the gas phase.

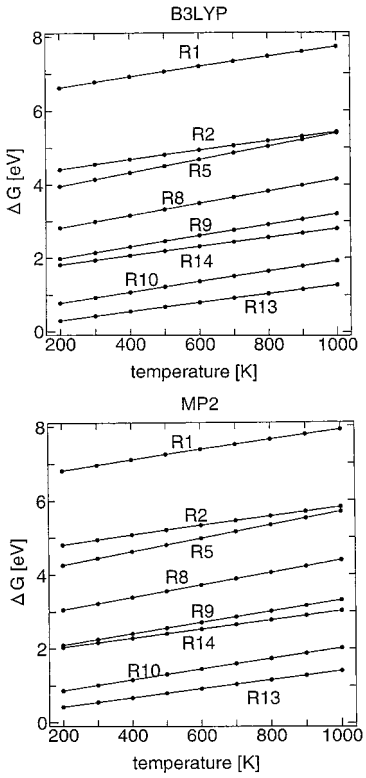

Figure 5. As in Figure 4 but for the Gibbs energy change of the reaction barrier (R1, R2, R5, R8−R10, R13, and R14).

Summary

Using ab initio molecular orbital theory, we examined CHF_3 decomposition and CHF_3 reactions with CHF_3 itself and its possible fragment species (CF_3, CHF_2, CF_2, CHF, CF, CH, F, and H). Although CHF_3 is widely used to etch SiO_2 films in the semiconductor industry, CHF_3 emitted from the etching process should not be allowed to escape to the atmosphere, as is the current practice, because of the strong greenhouse effect of the molecule. We focused particularly on polymerization and insertion reactions because an increased number of C atoms may facilitate collection of the CHF_3 molecule through a membrane separation technique. Although abstractions by radicals (CF_3, CHF_2, F, and H) occur with low reaction barriers, the polymerization of CHF_3 and insertion of a CF_2 radical have large reaction barriers. Only the insertions of CHF, CF, and CH radicals into C−H or C−F bonds seem to proceed in the gas phase.

Acknowledgment. We thank Drs. N. Sata, C. Shitara, and S. Samukawa for their useful discussions.

References and Notes

(1) Intergovernmental Panel on Climate Change (IPCC), The 1995 Working Report of the Scientific Assessment Working Group of IPCC.
(2) Samukawa, S.; Furuoya, S. *Appl. Phys. Lett.* **1993**, *63*, 2044.

(3) Karecki, S.; et al. *J. Electrochem. Soc.* **1998**, *145*, 4305.
(4) Beu, L. et al. International SEMATECH, Technology Transfer 1998, No. 98053508A-TR.
(5) Becke, A. D. *J. Chem. Phys.* **1993**, *98*, 1372.
(6) Becke, A. D. *Phys. Rev. A* **1988**, *38*, 3098.
(7) Vosko, S. H.; Wilk, L.; Nusair, M. *Can. J. Phys.* **1980**, *58*, 1200.
(8) Lee, C.; Yang, W.; Parr, R. G. *Phys. Rev. B* **1988**, *37*, 785.
(9) Petersson, G. A.; Bennett, A.; Tensfelde, T. G.; Al-Laham, M. A.; Shirley, W. A.; Mantzaris, J. *J. Chem. Phys.* **1988**, *89*, 2193. Petersson, G. A.; Al-Laham, M. A. *J. Chem. Phys.* **1991**, *94*, 6081.
(10) Scott, A. P.; Radom, L. *J. Phys. Chem.* **1996**, *100*, 16502.
(11) Curtiss, L. A.; Raghavachari, K.; Trucks, G. W.; Pople, J. A. *J. Chem. Phys.* **1991**, *94*, 7221.
(12) Curtiss, L. A.; Raghavachari, K.; Redfern, P. C.; Rassolov, V.; Pople, J. A. *J. Chem. Phys.* **1998**, *109*, 7764.
(13) Curtiss, L. A.; Redfern, P. C.; Raghavachari, K.; Rassolov, V.; Pople, J. A. *J. Chem. Phys.* **1999**, *110*, 4703.
(14) Frish, M. J.; Trucks, G. W.; Schlegel, H. B.; Gill, P. M. W.; Johnson, B. G.; Robb, M. A.; Cheeseman, J. R.; Keith, T. A.; Petersson, G. A.; Montgomery, J. A.; Raghavachari, K.; Al-Laham, M. A.; Zakrzewski, V. G.; Oritz, J. V.; Foresman, J. B.; Cioslowski, J.; Stefanov, B. B.; Nanayakkara, A.; Challacombe, M.; Peng, C. Y.; Ayala, P. Y.; Chen, W.; Wong, M. W.; Andres, J. L.; Replogle, E. S.; Gomperts, R.; Martin, R. L.; Fox, D. J.; Blinkley, J. S.; Defrees, D. J.; Baker, J.; Stewart, J. P.; Head-Gordon, M.; Gonzalez, C.; Pople, J. A. *Gaussian 94*; Gaussian, Inc.: Pittsburgh, PA, 1995.
(15) Frisch, M. J.; Trucks, G. W.; Schlegel, H. B.; Scuseria, G. E.; Robb, M. A.; Cheeseman, J. R.; Zakrzewski, V. G.; Montgomery, J. A.; Stratmann, R. E.; Burant, J. C.; Dapprich, S.; Millam, J. M.; Daniels, A. D.; Kudin, K. N.; Strain, M. C.; Farkas, O.; Tomasi, J.; Barone, V.; Cossi, M.; Cammi, R.; Mennucci, B.; Pomelli, C.; Adamo, C.; Clifford, S.; Ochterski, J.; Petersson, G. A.; Ayala, P. Y.; Cui, Q.; Morokuma, K.; Malick, D. K.; Rabuck, A. D.; Raghavachari, K.; Foresman, J. B.; Cioslowski, J.; Ortiz, J. V.; Stefanov, B. B.; Liu, G.; Liashenko, A.; Piskorz, P.; Komaromi, I.; Gomperts, R.; Martin, R. L.; Fox, D. J.; Keith, T.; Al-Laham, M. A.; Peng, C. Y.; Nanayakkara, A.; Gonzalez, C.; Challacombe, M.; Gill, P. M. W.; Johnson, B. G.; Chen, W.; Wong, M. W.; Andres, J. L.; Head-Gordon, M.; Replogle, E. S.; Pople, J. A. *Gaussian98*; Gaussian, Inc.: Pittsburgh, PA, 1998.
(16) Miyata, K.; Hori, M.; Goto, T. *J. Vac. Sci. Technol. A* **1996**, *14*, 2083.
(17) Miyata, K.; Hori, M.; Goto, T. *J. Vac. Sci. Technol. A* **1996**, *14*, 2343.
(18) Ricca, A. *J. Phys. Chem. A* **1999**, *103*, 1876.
(19) Optimized molecular geometries (reactants, products, and TSs) are available from the authour via e-mail (okamoto@frl.cl.nec.co.jp).
(20) Barin, I. *Thermochemical Data of Pure Substances*; VCH: Weinheim, Germany, 1989.